iScience, Volume *24*

Supplemental information

ATF6 aggravates angiogenesis-osteogenesis coupling during ankylosing spondylitis by mediating FGF2 expression in chondrocytes

Mengjun Ma, Hongyu Li, Peng Wang, Wen Yang, Rujia Mi, Jiahao Zhuang, Yuhang Jiang, Yixuan Lu, Xin Shen, Yanfeng Wu, and Huiyong Shen

Supplementary information titles and legends

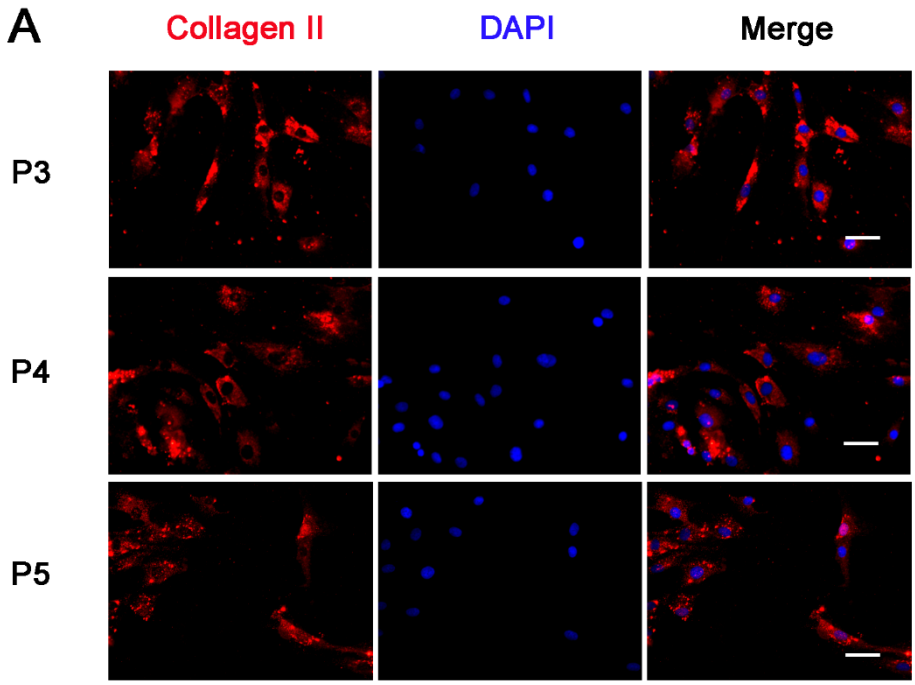

Figure S1. Expression of collagen II in chondrocytes, related to Figure 1.

(A) IHC staining for collagen II was performed on chondrocytes at passages 3-5. Scale bar, 50 μm.

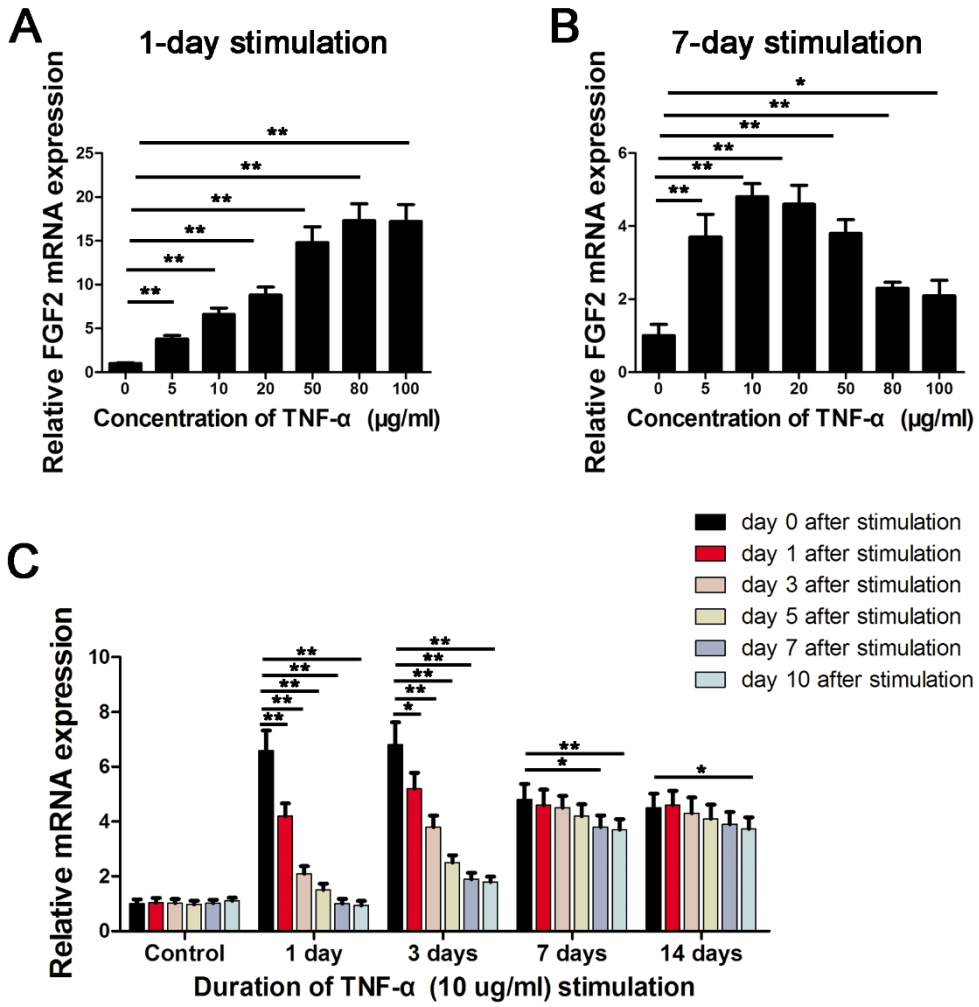

Figure S2. Seven-day treatment with a low concentration of TNF-α exerted a sustained effect on chondrocyte FGF2 expression, related to Figure 1.

(A) FGF2 mRNA levels were measured in chondrocytes treated with different concentrations of TNF-α for 1 day. (B) FGF2 mRNA levels were measured in chondrocytes treated with different concentrations of TNF-α for 7 days. (C) After treatment with 10 μg/ml TNF-α for a specific number of days (control, 1 day, 3 days, 7 days, or 14 days), chondrocytes were collected at 6 time points (day 0, day 1, day 3, day 5, day 7 and day 10) after treatment and RNA was extracted to determine FGF2 mRNA expression. Bars show the means ± SD.

*P<0.05 and **P<0.01, 2-tailed Student's t-test.

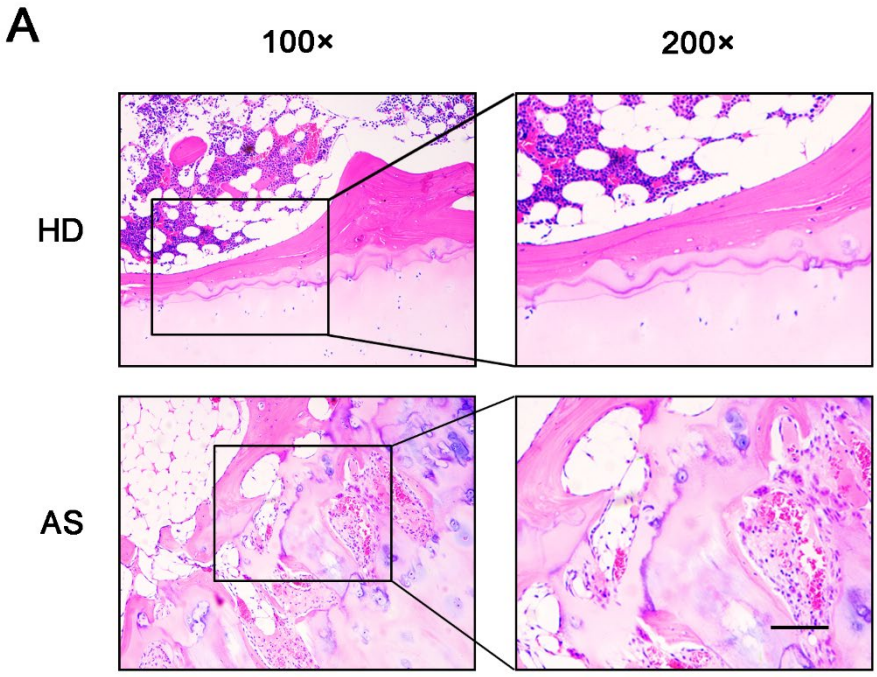

Figure S3. The cartilage structure in femur heads from patients with AS was destroyed by granulation tissue, related to Figure 1.

(A) H&E staining was performed on femur head cartilage from patients with AS. Scale bar, 100 μm.

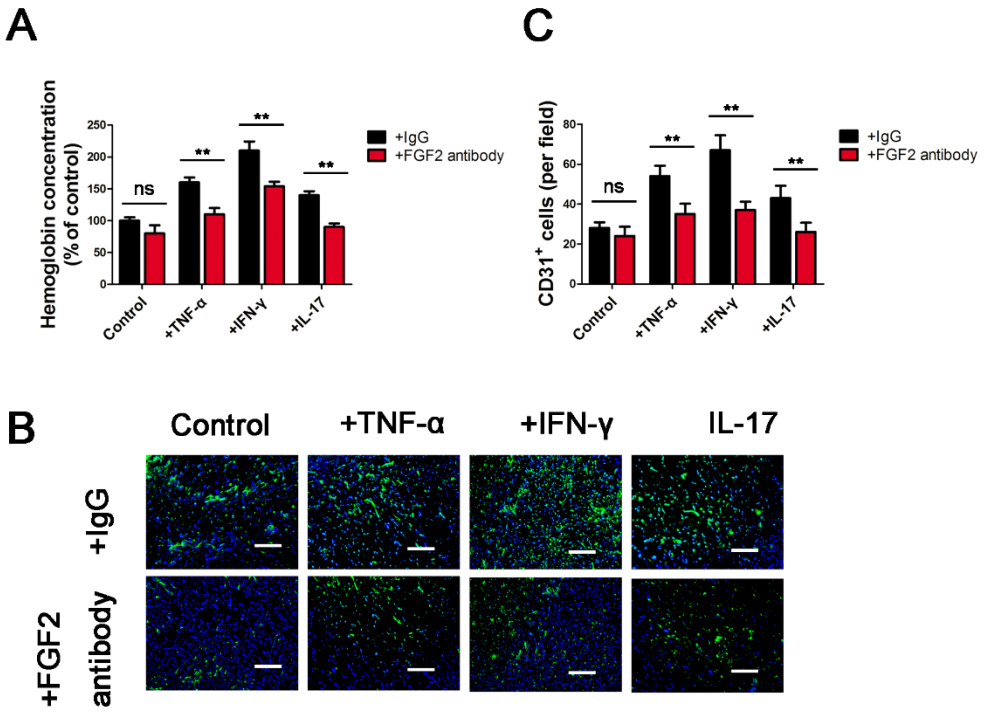

Figure S4. Chondrocytes secrete FGF2 to induce angiogenesis *in vivo*, related to Figure 3.

Matrigel plugs containing chondrocyte CM and TNF-α-treated chondrocyte CM with or without an FGF-2-neutralizing antibody were subcutaneously injected into nude mice. The plugs were collected on day 7. (A) Hemoglobin levels in the plugs were quantified and normalized to the control group (n = 6 mice per group). (B) Paraffin sections of Matrigel plugs were stained with the endothelial cell marker CD31. Scale bar, 100 μm. (C) CD31-positive cells were quantified. Bars show the means ± SD. *P<0.05 and **P<0.01, 2-tailed Student's t-test.

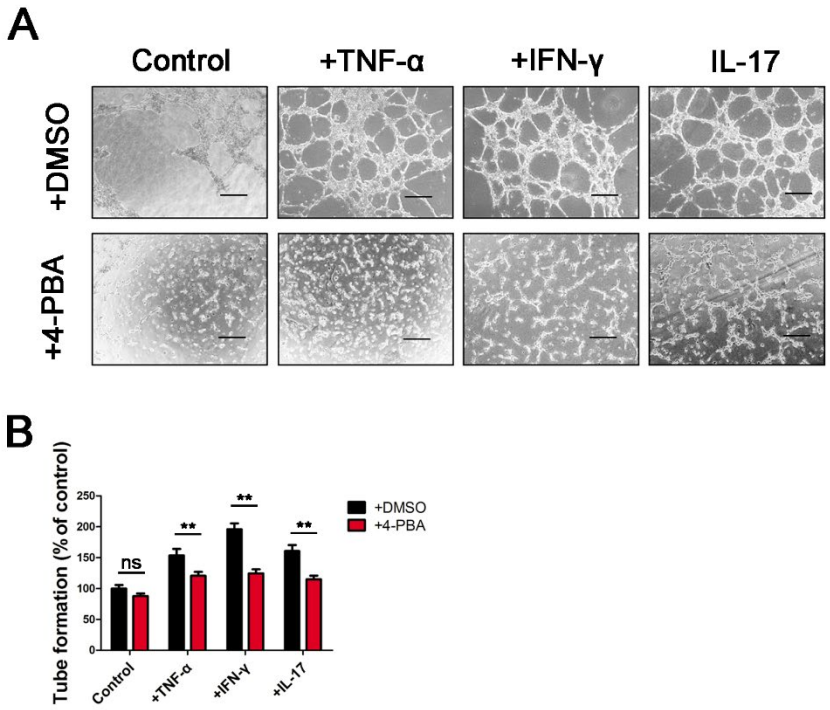

Figure S5. The ERS alleviator 4-PBA inhibited the angiogenic effect of chondrocytes, related to Figure 3.

(A&B) A tube-formation assay was performed on HUVECs cultured in CM (A). The number of branches was calculated and quantified using ImageJ software (B). Scale bar, 100 μm. Bars show the means ± SD. *P<0.05 and **P<0.01, 2-tailed Student's t-test.

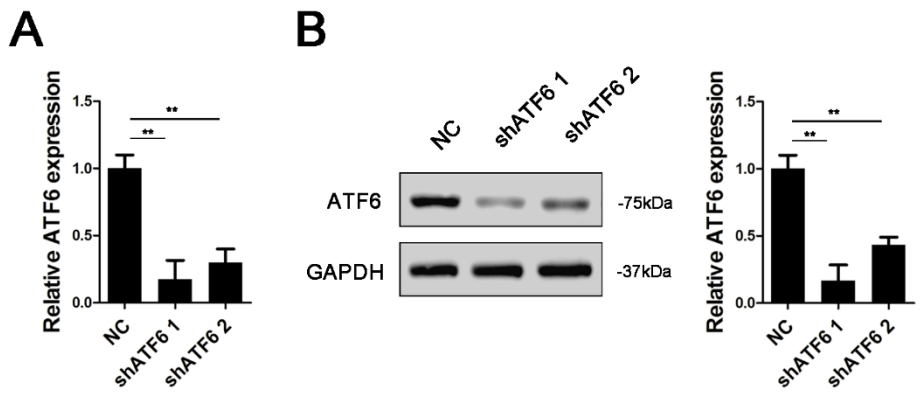

Figure S6. Knockdown of ATF6 expression in chondrocytes, related to Figure 4.

(A&B) qRT-PCR and WB measurement of ATF6 expression in chondrocytes. Bars show the means ± SD. *P<0.05 and **P<0.01, 2-tailed Student's t-test.

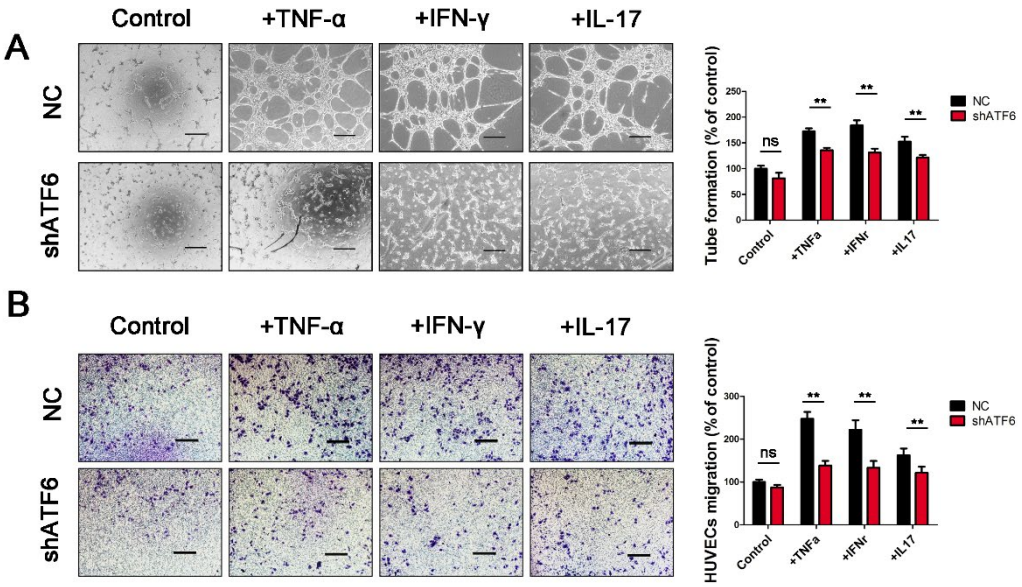

Figure S7. ATF6 knockdown inhibited the angiogenic effect of chondrocytes, related to Figure 4.

(A&B) Tube-formation assays and Transwell migration assays were performed on HUVECs cultured in CM. The numbers of branches and migratory cells were calculated and quantified using ImageJ software. Scale bar, 100 μm. Bars show the means ± SD. *P<0.05 and **P<0.01, 2-tailed Student's t-test.

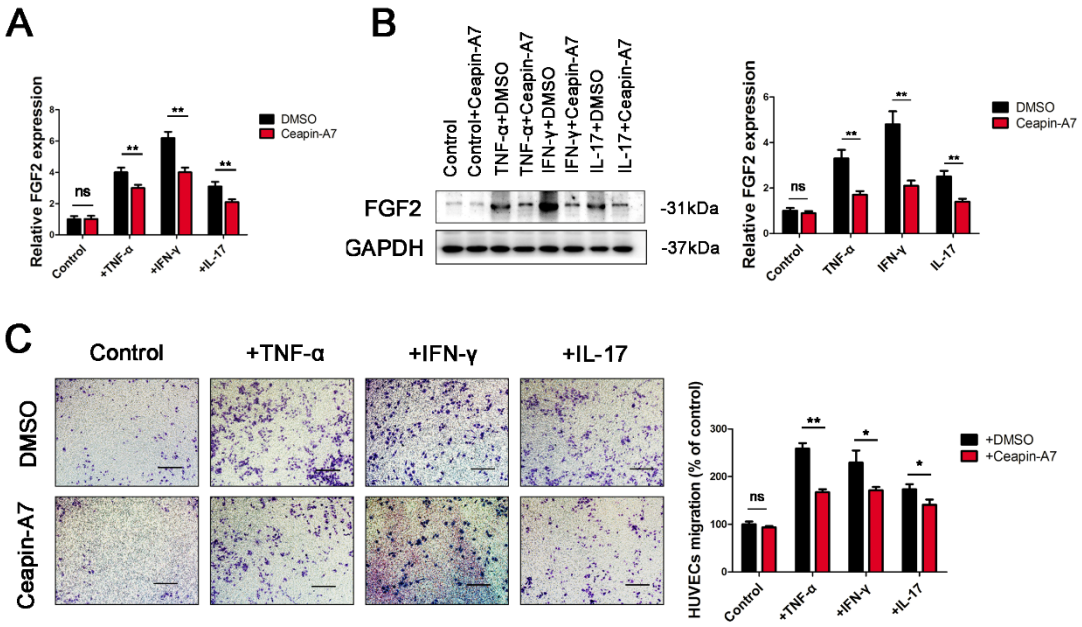

Figure S8. The ATF6 inhibitor Ceapin-A7 inhibited the angiogenic effect of chondrocytes, related to Figure 4.

(A&B) Levels of the FGF2 mRNA and protein in chondrocytes were measured after treatment with Ceapin-A7. (C) Transwell migration assays were performed on HUVECs cultured in CM. The number of migratory cells was calculated and quantified using ImageJ software. Scale bar, 100 μm. Bars show the means ± SD. *P<0.05 and **P<0.01, 2-tailed Student's t-test.

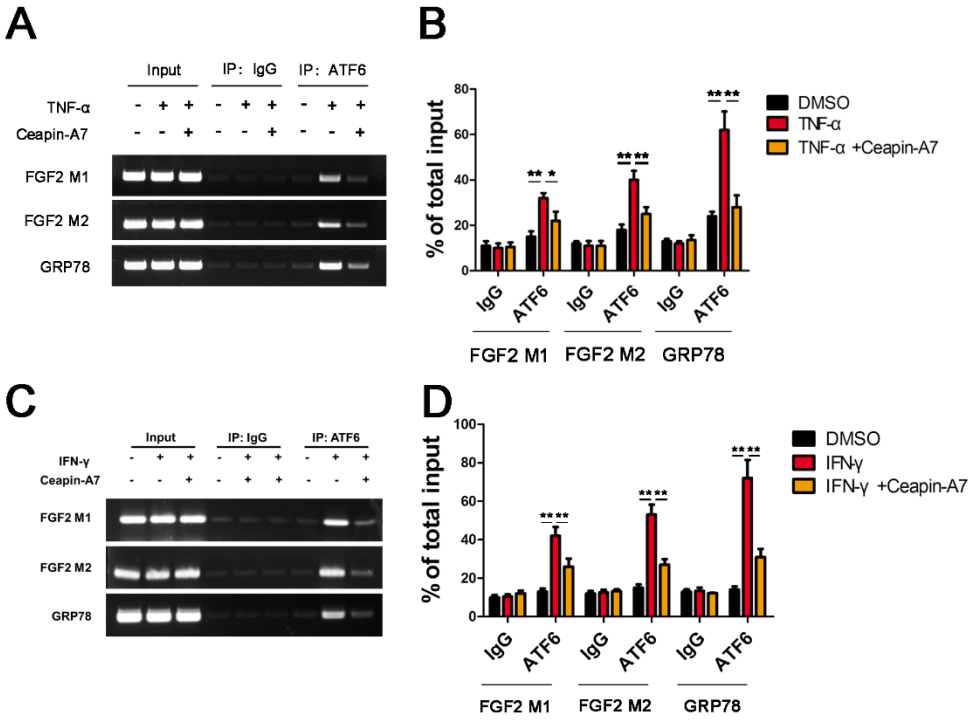

Figure S9. ATF6 binds to the human FGF2 promotor, related to Figure 5.

(A-D) After chondrocytes were treated with TNF-α and IFN-γ for 48 h, the ability of ATF6 to bind to the *FGF2* and *GRP78* promoters was analyzed using ChIP assays. Bars show the means ± SD. *P<0.05 and **P<0.01, one-way ANOVA followed by Dunnett's *post hoc* test.

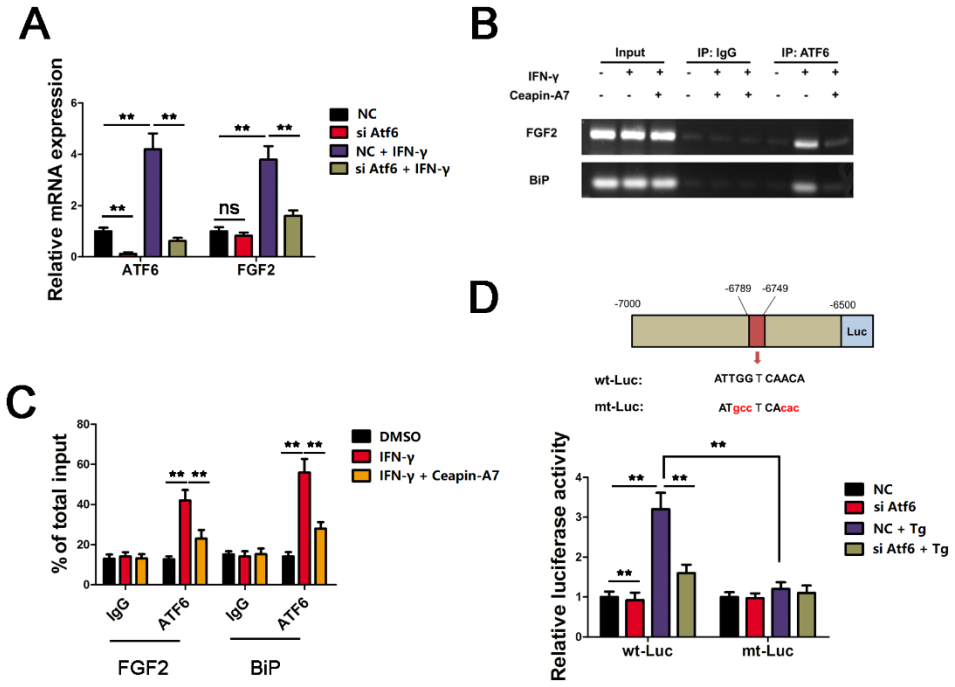

Figure S10. ATF6 binds to the mouse FGF2 promotor and promotes FGF2 expression, related to Figure 5.

(A) The expression of the *ATF6* and *FGF2* mRNAs was measured after ATF6 knockdown and IFN-γ treatment in the mouse chondrogenic cell line ATDC5. (B&C) After treatment with IFN-γ for 48 h, the ability of ATF6 to bind the mouse *FGF2* and *BiP* promoters in chondrocytes was analyzed using ChIP assays. (D) Diagram of the locations of ERSE in the mouse *FGF2* 5′-flanking region, their sequences (wt), and the mutations to those sequences (mt). ATDC5 cells were transfected with plasmids encoding mouse FGF2(−7000/-6500)-Luc wt or mt. Then, ATDC5 cells were treated with the ATF6 siRNA or the ERS inducer Tg. Forty-eight hours later, luciferase levels were measured in extracts. Bars show the means ± SD. *P<0.05 and **P<0.01, one-way ANOVA followed by Dunnett's *post hoc* test.

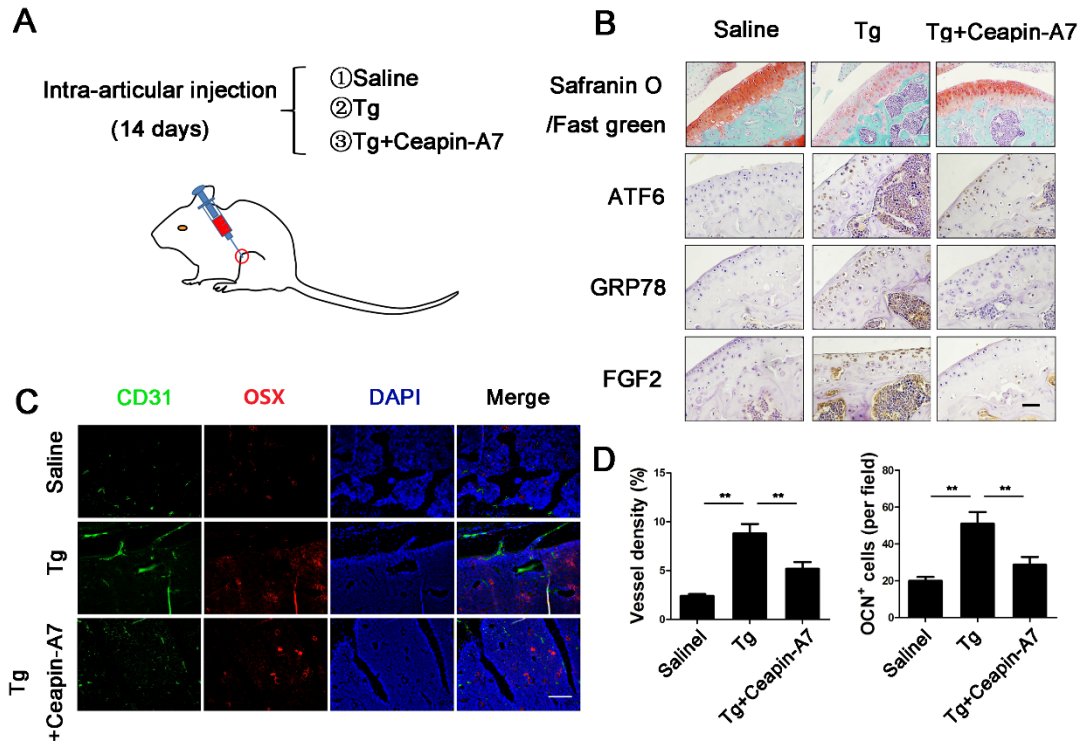

Figure S11. Ceapin-A7 inhibited ERS-induced FGF2 expression and osteogenesis in mice, related to Figure 6.

(A) Diagram of the intra-articular injection of saline, Tg or Tg+Ceapin-A7 in C57BL/6 mice for 2 weeks. (B) Safranin O/fast green staining of knee joints of treated mice showing articular cartilage degeneration. IHC staining for ATF6, GRP78 and FGF2 was performed on knee joints from C57BL/6 mice after treatment with saline, Tg or Tg+Ceapin-A7 for 2 weeks. Scale bar, 50 μm. (C) IF staining of knee joints from C57BL/6 mice showing endothelial cells (CD31+) and activated osteoblasts (OSX+) around knee joints. Scale bar, 50 μm. (D) Quantification of the proportions of CD31+ vessels and OSX+ cells. (n = 10 mice per group). Bars show the means ± SD. *P<0.05 and **P<0.01, one-way ANOVA followed by Dunnett's *post hoc* test.

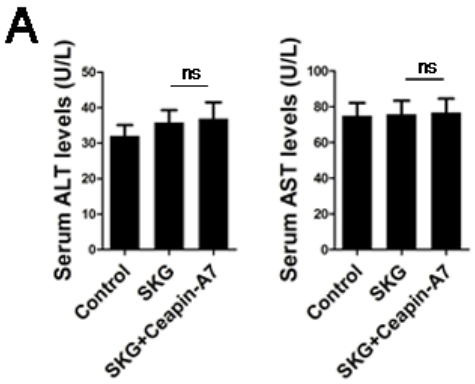

Figure S12. Ceapin-A7 did not cause liver damage in SKG mice, related to Figure 6.

(A) Serum levels of alanine amino transferase (ALT) and aspartate amino transferase (AST) were measured. (n = 10 mice per group). Bars show the means ± SD. *P<0.05 and **P<0.01, one-way ANOVA followed by Dunnett's *post hoc* test.

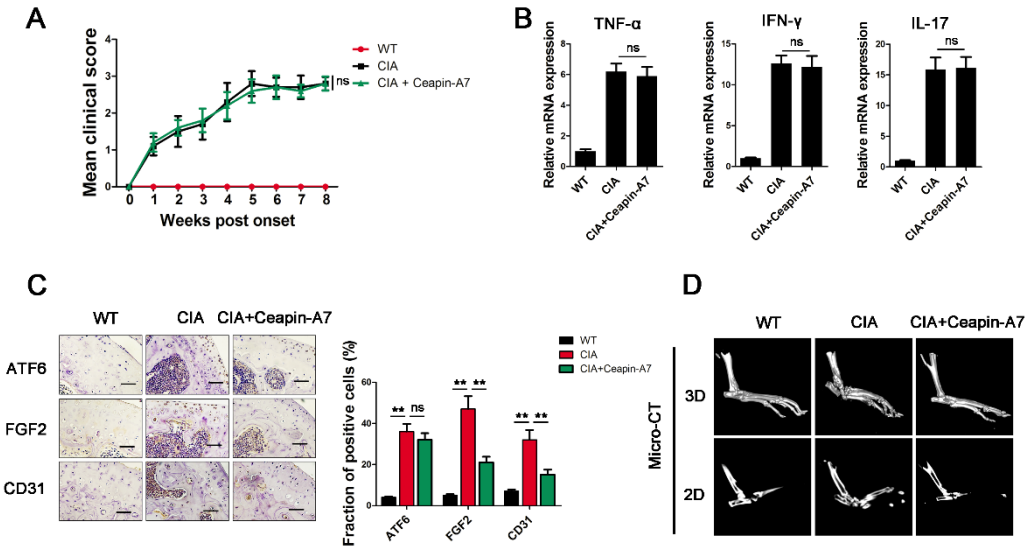

Figure S13. Ceapin-A7 inhibited FGF2 expression in the CIA model, related to Figure 6.

(A) Clinical scores were measured in SKG mice. (B) Local expression of the *TNF-α, IFN-γ* and *IL-17* mRNAs in the hind paws of CIA mice. (C) IHC staining for ATF6, FGF2 and CD31 in knee joints. ATF6-, FGF2-, CD31-positive cells were quantified. Scale bar, 50 μm. (D) Representative micro-CT images of ankles obtained from CIA mice in WT, 8 weeks after induction, and 8 weeks after induction and treatment with Ceapin-A7. (n = 10 mice per group). Bars show the means ± SD. *P<0.05 and **P<0.01, one-way ANOVA followed by Dunnett's *post hoc* test.

Table S1. Characteristics of the study subjects, related to STAR methods.

	Healthy donors	Patients with AS
Number	30	30
Age, years	28.5±8.5	27.9±9.1
Male, n (%)	16 (53.3%)	18 (60%)
Disease duration, years	NA	6.8±2.1*
BASDAI	0.9±0.4	4.5±1.5*

AS, ankylosing spondylitis; BASDAI, Bath Ankylosing Spondylitis Disease Activity Index. Data are presented as the means ± SD. *P<0.05, 2-tailed Student's t-test.

Table S2. Primer pairs used for qRT-PCR, related to STAR methods.

VEGF	F: 5'-AGGGCAGAATCATCACGAAGT-3' R: 5'-AGGGTCTCGATTGGATGGCA-3'
FGF2	F: 5'-AGAAGAGCGACCCTCACATCA-3' R: 5'-CGGTTAGCACACACTCCTTTG-3'
IGF-1	F: 5'-GCTCTTCAGTTCGTGTGTGGA-3' R: 5'-GCCTCCTTAGATCACAGCTCC-3'
EGF	F: 5'-TGGATGTGCTTGATAAGCGG-3' R: 5'-ACCATGTCCTTTCCAGTGTGT-3'
TGF-β	F: 5'-GGCCAGATCCTGTCCAAGC-3' R: 5'-GTGGGTTTCCACCATTAGCAC-3'
IL-6	F: 5'-ACTCACCTCTTCAGAACGAATTG-3' R: 5'-CCATCTTTGGAAGGTTCAGGTTG-3'
GAPDH	F: 5'-CTGGGCTACACTGAGCACC-3' R: 5'-AAGTGGTCGTTGAGGGCAATG-3'
GRP78	F: 5'-CATCACGCCGTCCTATGTCG-3' R: 5'-CGTCAAAGACCGTGTTCTCG-3'
GRP94	F: 5'-CCAGTTTGGTGTCGGTTTCTAT-3' R: 5'-CTGGGTATCGTTGTTGTGTTTTG-3'
IRE1	F: 5'-AGAGAAGCAGCAGACTTTGTC-3' R: 5'-GTTTTGGTGTCGTACATGGTGA-3'
PERK	F: 5'-GGAAACGAGAGCCGGATTTATT-3' R: 5'-ACTATGTCCATTATGGCAGCTTC-3'
ATF6	F: 5'-TCCTCGGTCAGTGGACTCTTA-3' R: 5'-CTTGGGCTGAATTGAAGGTTTTG-3'